

values of the population parameters for the best fits. Bertsch² has recently studied collective aspects of the calcium isotopes and succeeded in reproducing the empirical spectrum of ⁴²Ca rather well. He obtains a value of +0.12 for the $E2/M1$ mixing ratio for the $2_2^+ \rightarrow 2_1^+$ transition, which agrees quite well with our experimental value of $+0.20 \pm 0.10$.

B. ⁴⁴Ca

The level scheme for ⁴⁴Ca is shown in Fig. 3, and is based partially upon the recent MIT inelastic scattering work.¹³ The coincidence correlation data are shown in Figs. 9 and 10 with fits for spins 2 and 3 superimposed. The χ^2 plot is presented in Fig. 11. The value of the $E2/M1$ mixing ratio for the $2_2^+ \rightarrow 2_1^+$ transition is $+0.14 \pm 0.07$. It is rather interesting to note the close similarity between ⁴²Ca and ⁴⁴Ca. The $E2/M1$ ratios for the $2_2^+ \rightarrow 2_1^+$ transition is another piece of evidence for this similarity. The values of the population parameters corresponding to the best fits are listed in Table I.

¹³ T. A. Belote, W. E. Dorenbusch, and O. Hansen, *Bull. Am. Phys. Soc.* **10**, 539 (1965).

C. ⁴⁸Ti

The portion of the level scheme shown in Fig. 5 is consistent with the recent work¹⁴ at M.I.T. The correlation data are displayed in Figs. 12 and 13, and the χ^2 plot in Fig. 14. The best fit for the $2_2^+ \rightarrow 2_1^+$ transition occurs for an $E2/M1$ mixing ratio of -0.18 ± 0.09 . Table I lists the values of the population parameters corresponding to the best fit. Note the sign change as compared to the calcium isotopes. However, the magnitudes of the mixing ratios are about the same for all three of these transitions.

ACKNOWLEDGMENTS

The authors would like to thank Dr. R. N. Horoshko for assisting with the electronics. Thanks are due J. Ostrowski for preparing the calcium targets and W. Patton for programming assistance. The authors are grateful to Professor L. J. Lidofsky and Professor J. D. McCullen for stimulating discussions. Thanks are due Dr. G. F. Bertsch for unpublished reports of his work.

¹⁴ T. A. Belote, W. E. Dorenbusch, O. Hansen, and A. Sperduto, *Phys. Letters* **14**, 323 (1965).

Ar⁴⁰($p, p' \gamma$) Reaction Mechanism at Low Energies

H. HULUBEI, A. BERINDE, N. SCINTEI, N. MARTALOGU, I. NEAMU, AND C. M. TEODORESCU

Institute for Atomic Physics, Bucharest, Romania

(Received 15 April 1966)

The angular distributions of the protons inelastically scattered on Ar⁴⁰ at the bombardment energies of 4.1 and 7.3 MeV were measured with semiconductor detectors. The angular distribution at $E_p=4.1$ MeV, corresponding to the first excited state $Q=-1.46$ MeV of Ar⁴⁰, and the angular distributions at $E_p=7.3$ MeV on the higher excited states of the target are well explained by the statistical model of the compound nucleus with the inclusion of the (p, n) outgoing channels in the calculation. The angular distribution at $E_p=7.3$ MeV on the first excited state of Ar⁴⁰ shows a forward peak characteristic of the direct-interaction mechanism. The part taken by the direct interaction in the excitation of the first level of Ar⁴⁰ is confirmed by the ($p, p_1 \gamma$) angular correlations measured at $E_p=5.8$ MeV. An attempt is made to separate the contributions of the two reaction mechanisms to the excitation of the first excited state of Ar⁴⁰, in the 3-17-MeV bombardment-energy range. The spins for some levels of Ar⁴⁰ are also suggested.

INTRODUCTION

THE inelastic scattering of protons on Ar⁴⁰ has been the object of a number of experimental investigations.¹⁻⁵ The angular distribution of protons leaving Ar⁴⁰ in its first excited state was especially well studied. These distributions show a forward peak in the whole energy range studied (5.2-16.9 MeV), which constitutes

a characteristic feature of the direct-interaction (DI) process. At energies of 14.1 and 16.9 MeV the calculations performed on the basis of the distorted-wave Born approximation (DWBA) formalism explain well the experimental angular distributions.⁵ The fact that the direct-interaction process can be detected even at energies smaller than 7 MeV is probably due to a small contribution of the compound-nucleus (CN) mechanism. This small CN contribution may be related to the low (p, n) threshold (-2.29 MeV), the neutron outgoing channels representing a way of disintegration competing with the inelastic scattering of protons. On the other hand, the shape stability of the angular

¹ R. M. Eisberg and N. M. Hintz, *Phys. Rev.* **103**, 645 (1956).

² Y. Oda *et al.*, *J. Phys. Soc. Japan* **15**, 760 (1960).

³ H. Taketani and W. P. Alford, *Nucl. Phys.* **32**, 430 (1962).

⁴ H. Hulubei *et al.*, *Rev. Roum. Phys.* **8**, 107 (1963).

⁵ W. S. Gray, R. A. Kenefick, and J. J. Kraushaar, *Nucl. Phys.* **67**, 542 (1965).

distributions shows that the compound-nucleus contribution may be described by the statistical model. To specify the competition between the DI and the CN reaction mechanisms, in the present work we measured the (*p*, *p'*) angular distributions on Ar⁴⁰ at 4.1 and 7.3 MeV. To confirm the presence of the DI mechanism at low energies, the (*p*, *p'*γ) angular correlation at 5.8 MeV was measured. In the interpretation of the data, special attention is given to the competitive (*p*, *n*) outgoing channels.

THEORY

The experimental data are compared with the statistical-model predictions, and the deviations from this model are interpreted by the DI mechanism. Barvard and Kim⁶ showed that at 3.4-MeV proton bombardment energy, corresponding to about 11-MeV compound-nucleus excitation energy, the number of excited levels in the K⁴¹ compound nucleus is relatively high, above 40 levels/MeV. It is expected that our proton beam with an energy spread of 1% should satisfy the averaging condition necessary for the applicability of the statistical model. To calculate the inelastic cross section in the framework of the statistical model, we used Auerbach and Moore's⁷ formulas, based on Hauser and Feshbach's⁸ formalism. In the case of protons inelastically scattered on the spin-*I* excitation state of a nucleus having a 0⁺ ground state, the differential cross section can be written

$$\sigma(\theta) = \frac{1}{2}\lambda^2 \sum (-)^I (2J+1) Z(lj'l'j; \frac{1}{2}k) \times Z(l'j'l'j'; \frac{1}{2}k) W(Jj'Jj'; Ik) \tau P_k(\cos\theta). \quad (1)$$

Here the summation is performed over the spins *J* of the compound nucleus; over the orbital angular momenta *l*, *l'* of the incident protons of energy *E* and of the emergent protons of energy *E'*, respectively; over the total angular momenta *j* and *j'*; and over *k* which takes only even values. *Z* is the Blatt and Biedenharn⁹ coefficient, *W* is a Racah coefficient, *P_k* is a Legendre polynomial, and *τ* is

$$\tau = T_{ij}(E) T_{l'j'}(E') / \sum_{iE} T_{ij}(E), \quad (2)$$

where *T_{ij}* are the transmission coefficients, the summation being performed over all the disintegration channels of the compound nucleus consistent with the conservation of angular momentum. The energy dependence of the differential cross section and the influence of the competitive channels are included in *τ*.

The total inelastic cross section corresponding to the state of spin *I* is calculated by means of the formula

$$\sigma = \frac{1}{2}\pi\lambda^2 \sum (2J+1)\tau, \quad (3)$$

the summation including *J*, *l*, *l'*, *j*, and *j'*.

The calculation of the *p*₁–γ angular correlation function predicted by the statistical model was made by using the formula given by Sheldon,¹⁰ which in the case of the inelastic scattering on the first excited state *I* = 2⁺ is

$$W(\theta_p, \theta_\gamma, \varphi) = \frac{5\lambda^2}{32\pi} \sum \delta(\pm) (-)^{J+j'} (2J+1)^2 \times (2j'+1) (JJ\frac{1}{2}-\frac{1}{2}|\mu 0) (j'j'\frac{1}{2}-\frac{1}{2}|\nu 0) \times (221-1|\lambda 0) X(JJ\mu; j'j'\nu; 22\lambda) \tau S_{\mu\nu\lambda}(\theta_p, \theta_\gamma, \varphi), \quad (4)$$

where the sum is extended over *μ*, *ν*, *λ*, *J*, and *j'*; (*j₁j₂m₁m₂ | jm*) is the Clebsch-Gordan coefficient; *X* is the 9–*j* Wigner symbol; and *S_{μνλ}* are the Legendre hyperpolynomials.¹⁰ The symbol *δ*(±) excludes the interference between *j'* = *l'* + ½ and *j'* = *l'* – ½. The system of coordinates is taken with the *z* axis along the direction of the incident beam and the *y* axis along the normal to the reaction plane formed by the directions of the incident and emergent protons; *θ_p* is the angle of the scattered protons; *θ_γ* is the angle of emission of the γ radiation, and *φ* is the azimuthal angle.

In the numerical calculation the average transmission coefficients *T_l* = *T_{l, l+1/2}* = *T_{l, l-1/2}* were used. These were extracted by interpolation from Meldner and Lindner's¹¹ graphs. The calculation of the angular distribution and of the total inelastic cross section was carried out in the *l* ≤ 3 approximation for incident protons and the *l'* ≤ 2 approximation for emergent protons and neutrons.

In the angular-correlation case it was assumed that *l, l'* ≤ 2. The calculation of *τ* requires the knowledge of the spins and parities of the levels populated by (*p, p'*) and (*p, n*) reactions. The levels of Ar⁴⁰ populated by the reaction (*p, p'*), with spins and parities proposed by Gray *et al.*,⁶ were taken into consideration. Concerning the (*p, n*) channels, it must be emphasized that the K⁴⁰ residual nucleus has a very rich level diagram.¹² Only 9 out of the 54 levels of the diagram have known spins and parities. For a great part of the remaining levels, the possible parameters could be determined by using the values of the angular momentum transfer in the K³⁹(*d, p*)K⁴⁰ stripping reaction, studied by Enge *et al.*¹³ It was assumed that the rest of the levels could have spins and parities from 0± to 6±. Of all the possible values of the spins and parities, the ones used in the calculation were chosen by drawing lots. This operation was repeated three times, obtaining for each *τ* a set of three values, the maximum difference between them being 25%. But the inelastic total cross sections for the excitation of the first 2⁺ state of Ar⁴⁰, when the three sets of *τ* values were used, were different by less than 15%. Because of the large number of levels populated by the (*p, n*) reaction, the errors made in assigning

⁶ A. C. L. Barvard and C. C. Kim, Nucl. Phys. **28**, 428 (1961).

⁷ E. H. Auerbach and S. O. Moore, Phys. Rev. **135**, B895 (1964).

⁸ W. Hauser and H. Feshbach, Phys. Rev. **87**, 366 (1952).

⁹ J. M. Blatt and L. C. Biedenharn, Rev. Mod. Phys. **24**, 258 (1952).

¹⁰ E. Sheldon, Rev. Mod. Phys. **35**, 795 (1963).

¹¹ H. Meldner and A. Lindner, Z. Physik **180**, 362 (1964).

¹² P. M. Endt and C. Van der Leun, Nucl. Phys. **34**, 1 (1962).

¹³ H. A. Enge *et al.*, Phys. Rev. **115**, 949 (1959).

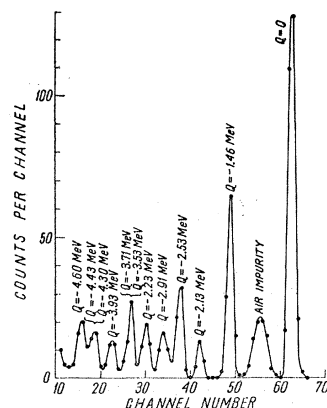


FIG. 1. Spectrum of the protons scattered on the Ar^{40} target, obtained at 7.3-MeV bombarding energy and angle $\theta = 100^\circ$.

values to the spin and parity of a level do not affect the cross-section values too much. It is likely that calculations made with precise knowledge of the parameters of each level of K^{40} could not make essential modifications in the cross sections calculated following the above procedure. It must be mentioned also that consideration of the (p,n) channels even so approximately as described above is decisive in bringing the theoretical cross section, calculated with the aid of the statistical model, close to the experimental cross section.

EXPERIMENTAL METHOD

The proton source was the cyclotron of the Institute for Atomic Physics in Bucharest. The angular distribution and correlation chambers were described in an earlier paper.¹⁴ The natural argon gaseous target at 150-mm Hg pressure was contained in a 6-cm diam cylindrical chamber provided with two windows for the entrance and exit of the beam, and two lateral windows which allowed the angular-distribution measurements in the 30° – 150° angular range. The windows of the target chamber were covered by a Mylar foil. The beam was collected by a Faraday cup. The angular distributions were measured by means of a surface-barrier silicon detector. A rectangular front slit and a circular opening at the detector defined the geometrical factor calculated by means of Silverstein's¹⁵ formula. The energy resolution for the elastic peak at 7.3 MeV was 2.5%. The pulses of the detector were amplified by a charge-sensitive preamplifier and introduced into a 400-channel pulse-height analyzer. A scintillation counter placed at an angle of 90° was used as monitor.

The correlation chamber allowed the simultaneous measurement of three correlation curves corresponding to the angles $\theta_p = 60^\circ$, 90° , and 120° of the proton detectors and to the azimuthal angle $\varphi = \pi$. The proton detectors used in the correlation experiment consisted of a 0.8-mm-thick $\text{CsI}(\text{Tl})$ crystal and a EMI-6097 photomultiplier. As a gamma-radiation detector, a 3.8-cm-diam and 2.5-cm-high $\text{NaI}(\text{Tl})$ crystal mounted

on an EMI-9537 photomultiplier was used. The coincidences were measured by means of an electronic circuit including three fast-slow coincidence systems,¹⁴ each having a resolving time of 25 nsec. The coincident and noncoincident proton spectra were recorded by means of a 400-channel pulse-height analyzer. The random coincidences were evaluated using the two spectra and the fact that the elastic peak of the coincident spectrum cannot contain true coincidences.

In the experiment at 4.1 MeV the energy of the incident proton beam was measured by means of the "crossover" kinematic technique,¹⁶ which involves seeking the angle at which the protons scattered on the first excited state, and in turn on the groups formed by the second and the third excited states of Ti^{48} , have the same energy as the protons scattered on hydrogen. The energy of the 7.3-MeV protons was determined also by a kinematic method,¹⁷ consisting of the measurement of the angles at which the protons inelastically scattered on every two consecutive excited states of Ar^{40} have equal energies. The energy of the 5.8-MeV protons used in the separated angular-correlation experiment has been measured by the method of total absorption in Al foils.

RESULTS AND DISCUSSION

A typical spectrum of Ar^{40} obtained at 7.3 MeV is shown in Fig. 1. The excitation energies were assigned using the Ar^{40} level diagram given by Gray *et al.*⁵ and the calibration curve drawn by means of the elastic peak and of the first three inelastic peaks using the kinematics of the reaction and the corrections due to the target thickness. The angular distributions of the protons scattered on the 2^+ ($Q = -1.46$ MeV) first excited state of Ar^{40} at $E_p = 4.1$ and 7.3 MeV are shown in Fig. 2. The relative errors on the curves represent the sum of the statistical errors and of the uncertainty in estimating the background. The error in the absolute-cross-section measurements was estimated to 10%. These distributions are compared with the statistical-model predictions. The theoretical calculation was carried out by means of formula (1). At the energy $E_p = 4.1$ MeV, the difference among the three sets of values of the τ coefficients is negligible, reflecting the fact that the open (p,n) channels lead to the K^{40} levels with known spins and parities. At $E_p = 7.3$ MeV, three theoretical angular-distribution curves were obtained, corresponding to the three sets of τ values. The shapes of the three curves are practically the same, differing only by the absolute value of the differential cross section, the maximum difference being 13%. The average of these three curves is shown in Fig. 2. As can be seen, at the energy 4.1 MeV, the statistical model explains well the shape and the absolute value of the experimental differential cross section. If we do not

¹⁴ H. Hulubei *et al.*, Phys. Rev. **139**, B871 (1965).

¹⁵ E. A. Silverstein, Nucl. Instr. Methods **4**, 53 (1959).

¹⁶ B. M. Bardin and M. E. Rickey, Rev. Sci. Instr. **35**, 902 (1964).

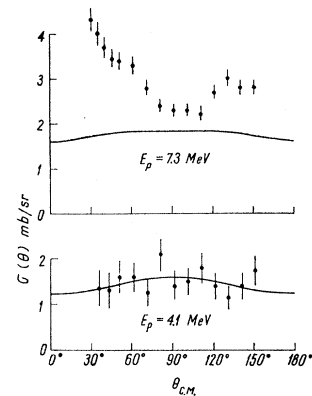
¹⁷ H. Hulubei *et al.*, Compt. Rend. **262**, 1351 (1966).

take into consideration the competition of the (*p*,*n*) channels, we obtain a differential cross section approximately six times greater than the measured one. This suggests that the statistical model can describe the inelastic proton scattering on Ar⁴⁰ at this energy, provided that the (*p*,*n*) channels are taken into consideration. Used in this way the statistical model also describes the (*p*,*p*₁γ) angular correlation at this energy.¹⁸ We notice that at $E_p = 4$ MeV, the presence of the (*p*,*n*) reaction changes not only the absolute value, but also the shape of the angular correlation.¹⁸

The angular distribution obtained at the energy 7.3 MeV is in agreement with the predictions of the statistical model. It is characterized by a forward peak. Similar distributions were also observed at other energies in the range of 5.2–16.9-MeV.^{1–5} The forward peak suggests the presence of a direct-interaction mechanism. At 7.3 MeV and also probably at the other energies the DI mechanism is in competition with the CN mechanism described by the statistical model. By subtracting the CN curve calculated by means of the statistical model from the experimental distribution, the contribution to the reaction of the DI mechanism can be obtained. Such an attempt will be made in the present work. For this we must have full confidence in the applicability of the statistical model to the description of the CN contribution at 7.3 MeV and eventually at the other energies. We saw that at $E_p = 4.1$ MeV this model operates well enough. We are expecting that at 7.3 MeV, the direct-interaction contribution will be negligible in the (*p*,*p'*) excitation of the higher Ar⁴⁰ levels. This fact has been shown by Kokame and Fukunaga¹⁹ in the case of the (*p*,*p'*) reaction on Al²⁷. These authors have shown that the angular distribution on the protons scattered on the fourth excited state of Al²⁷ is symmetrical about 90°, while the angular distributions on the first excited states present symmetries partially attributed to the DI process. Assuming that the CN-process cross section is proportional to $2I+1$, Kokame and Fukunaga succeeded in separating the contribution of the two competing mechanisms to the excitation through inelastic scattering of the other levels of Al²⁷.

The angular distributions on the higher excited states of Ar⁴⁰ are shown in Fig. 3. Beginning with the state $Q = -2.91$ MeV, these distributions are practically isotropic, which suggests the dominance of the CN mechanism. They are compared with the solid curves provided by the statistical model, obtained by averaging the three sets of τ values. The agreement between theory and experiment is good enough. The angular distribution for the 2.13-MeV state is close to the shape and to the absolute value of the theoretical differential cross section calculated on the hypothesis of the 0+ spin and parity. The increase of the differential cross

FIG. 2. The angular distributions of the protons inelastically scattered on the first 2+ state of Ar⁴⁰ ($Q = -1.46$ MeV). The solid curve was computed on the basis of the statistical model.



section at small angles can be attributed to the DI mechanism. A similar distribution as regards the form has been observed at lower energies.^{3,4} The spin and parity of the 2.13-MeV state has been determined as 0+ through (*p*,*p'*γ) and γ-γ angular-correlation experiments by Wakatsuki *et al.*²⁰ at $E_p = 5.6$ MeV. Concomitantly with the (*p*,*p*₁γ) angular correlation on the first excited level at $E_p = 5.8$ MeV, we have obtained also the (*p*,*p*₂γ) angular correlation between the protons inelastically scattered on the second excited level and the second gamma rays of the 0+ → 2+ → 0+ cascade. The isotropy obtained confirms the 0+ spin attributed to the 2.13-MeV level. Wakatsuki *et al.*²⁰ have also obtained isotropy, but between protons inelastically scattered on the second excited state of Ar⁴⁰ and the first gamma radiation of the 0+ → 2+ → 0+ cascade.

The angular distribution on the 2.53-MeV state is not inconsistent with the spin and parity 2+, assigned by Mathur and Morgan,²¹ if we attribute the increasing of the differential cross section at about 70° to the DI process. Gray *et al.*⁵ have assigned a 4+ spin to the 2.91-MeV state. The present experiment is in agreement with this assignment. The curve predicted by the spin 3+ is entirely above the experimental points. Since in the case of the first excited states the experimental points tend to be situated above the theoretical curves, a fact attributed to the direct interaction, the possibility of a 3+ spin for the 2.91-MeV state can be considered inconsistent with our experimental data. The present data contradict the 4+ assignment²¹ for the 3.23-MeV level, suggesting a 2+ value. The 3.53- and 3.71-MeV states have not been resolved in the present experiment. The spin and parity of the 3.71-MeV state are known to be 3-. The theoretical curves of Fig. 3 represent the sum of the differential cross section corresponding to this state and the differential cross section for the 3.53-MeV state, supposing for the latter 1+ and 2+ spin-parity, respectively. The fit is likewise good in both cases. The present data do not contradict the 2±

¹⁸ H. Hulubei *et al.*, Phys. Letters **19**, 675 (1966).

¹⁹ J. Kokame and K. Fukunaga, J. Phys. Soc. Japan **20**, 649 (1965).

²⁰ T. Wakatsuki, Y. Hirao, and I. Miura, Nucl. Phys. **39**, 335 (1962).

²¹ S. C. Mathur and I. L. Morgan, Nucl. Phys. **73**, 579 (1965).

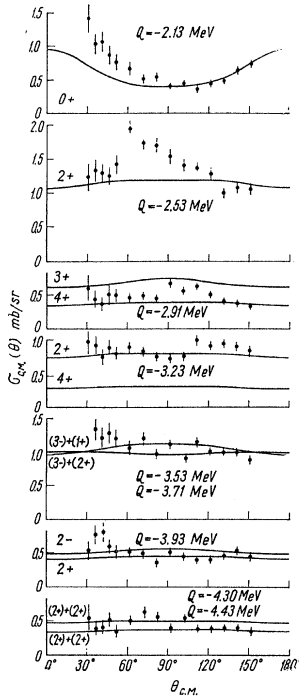


FIG. 3. The inelastic angular distributions on Ar^{40} at 7.3-MeV bombarding energy. The solid curves show the predictions of the statistical model.

spin assignment⁵ for the 3.93-MeV state. For the 4.30- and 4.43-MeV states, combinations with various spins were taken into consideration, keeping unchanged the spin 2+ for the 4.43-MeV state suggested by Gray *et al.*⁵ The best agreement was obtained with the spins 2+ and 3+ for the 4.30-MeV state. A similarly good fit was obtained by taking into consideration states with negative parity.

In Fig. 4 a level scheme of Ar^{40} is suggested. The position of the levels was established on the basis of the work of Gray *et al.*⁵ If we consider the $Q = -3.71$ -MeV state as the first excited state, with negative parity, all the lower levels have positive parities. It is interesting to notice that the spins and parities suggested for the 2.91- and 3.23-MeV levels are in accord with Iwao's²² theoretical calculation, which predicts a doublet at 2.94 and 2.95 MeV with the spin parities 4+ and 2+, respectively.

The agreement between the experimental data and the predictions of the statistical model, in the case of some of the higher excited states whose spins and parities were known before, confirms the validity of the approximations carried out in the calculation by the statistical model of the CN contribution as regards the first excited state. It is important to notice that the CN differential cross section has a maximum at a 90° angle, while the experimental data show here a minimum, as can be seen in Fig. 2, and hence the DI contribution has a minimum. In this case the experimental excitation function for the differential cross section at 90°, corresponding to the first excited state of Ar^{40} ,

should be close enough to the statistical-model predictions. This supposition is confirmed in Fig. 5, where the excitation function at 90° calculated on the basis of the statistical model is compared with the data in the literature. The calculation was performed up to a bombarding energy of 10 MeV, using the three sets of values for τ . The shape of the experimental curve is reproduced by the theoretical calculation, but the experimental points are situated in general above the theoretical curve because of the contribution of the DI mechanism. In order to confirm the existence of the DI mechanism at low energies with supplementary data, the $(p, p_1\gamma)$ angular correlation was measured at 5.8-MeV bombardment energy for three fixed angles of the proton detectors, $\theta_p = 60^\circ, 90^\circ,$ and 120° , the angle of the gamma-radiation detector varying in the 30° – 150° range. The measurements were made for azimuthal angle $\varphi = \pi$, i.e., with the proton and gamma detectors in the same plane with the beam, on either side of the latter.

The DWBA theory neglecting the proton spin flip in the reaction predicts a correlation function of the form

$$W(\theta_p, \theta_\gamma, \pi) = a + b \sin^2(\theta_\gamma - \theta_0), \quad (5)$$

where θ_0 is the symmetry axis of the correlation function. When the wave functions which describe the incident and emergent protons are approximated by plane waves, we have $a=0$ and $\theta_0 = \theta_R$, where θ_R is the classical recoil angle of the nucleus. An important characteristic of the correlation function (5) is the period of $\pi/2$ in contrast to the function (4) with a period of π , predicted by the statistical model.

The experimental data and theoretical curves predicted by the two reaction mechanisms are shown in Fig. 6.

The solid curves represent the DI-mechanism predictions and the dashed curves were calculated on the basis of the statistical model, using the formula (4) with averaged τ values.

In this figure are given also the expressions obtained by fitting the function (5) to the experimental data.

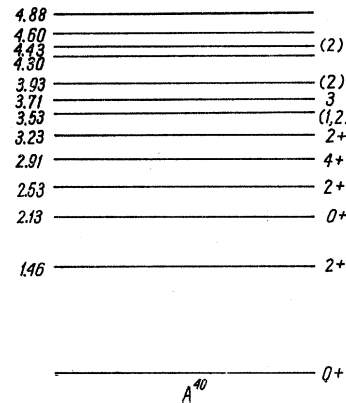


FIG. 4. Suggested level scheme for Ar^{40} .

²² S. Iwao Nucl. Phys. 42, 46 (1963).

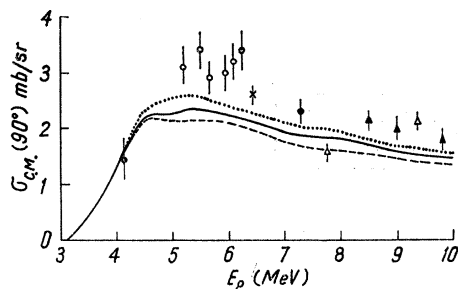


FIG. 5. The excitation function of the inelastically scattered protons on the 2+ excited state of Ar⁴⁰ ($Q = -1.46$ MeV) at $\theta = 90^\circ$. The theoretical curves represent the predictions of the statistical model, using three sets of τ values. ●—present results. ○—previous results (Ref. 4). X—Taketani and Alford (Ref. 3). △—Oda *et al.* (Ref. 2). ▲—Eisberg and Hintz (Ref. 1).

The formula (4) allows the calculation of the double differential absolute cross section, in contrast with the DI formula (5) which gives only the shape of the correlation curves. This makes possible the interpretation of the experimental data in terms of the relative values of the number of coincidences for various proton angles. In our case this comparison can be made, since the angular correlations were measured simultaneously at the three scattering angles, with practically the same geometrical conditions and detection efficiency. The CN theoretical correlation curve was normalized to the experimental data at $\theta_p = 90^\circ$, since the DI is at a minimum here. The CN theoretical curves, corresponding to 60° and 120° angles, were multiplied by the same normalization factor.

The theoretical curves calculated neglecting the (*p*,*n*) channels have practically the same form at this energy. The agreement with the curves predicted by the statistical model is poor, in contrast with the fit obtained by the DI curve, thus suggesting the presence of the direct process. This conclusion is supported also by the fact that at $\theta_p = 60^\circ$ the number of coincidences is almost double that from 90° and 120° . Also, at this angle the ratio b/a is greater than at the other scattering angles of the protons, which constitutes an argument in favor of a DI that is greater at 60° than at 90° and 120° . The symmetry axis of the experimental curves at supplementary angles $\theta_p = 60^\circ$ and 120° is situated very near the recoil angle of the nucleus. In the case of $\theta_p = 90^\circ$ the θ_0 symmetry axis differs from the recoil angle by approximately 16° .

In general, the experimental angular-correlation data are consistent with a competition between the two reaction mechanisms. The compound-nucleus mechanism shows itself through a reduction of the b/a ratio in comparison with the pure direct-interaction case. The essential fact, which permits us to put in evidence the DI mechanism in this case, is the reduced weight of a CN mechanism due to the (*p*,*n*)-channel competition. A similar situation was reported by Szostack and Gobbi²⁸

²⁸ R. Szostack and B. Gobbi, *Helv. Phys. Acta* **37**, 30 (1964).

in the (*p*,*p'*γ) angular-correlation study of the first excited state of Zn^{64,66,68} isotopes at 5.8-MeV energy.

For the Zn⁶⁴ and Zn⁶⁶ isotopes, whose (*p*,*n*) threshold is situated above the bombarding energy, the CN mechanism is predominant; but in the Zn⁶⁸ case, with a low (*p*,*n*) threshold ($Q = -3.7$ MeV), the reaction is dominated by the DI mechanism. It is to be noticed that in this case also the symmetry axis of the correlation at $\theta_p = 90^\circ$ differs strongly from the recoil angle, while at $\theta_p = 45^\circ$ and 135° , θ_0 is very close to θ_R .

In conclusion, the present data show that the approximations made in the CN cross-section evaluation nevertheless permit a satisfactory fit to the experimental data of the angular distribution at $E_p = 4.1$ MeV for the first excited state of Ar⁴⁰, and at $E_p = 7.3$ MeV for the higher excited states of Ar⁴⁰. Also, the general aspect of the excitation function of the experimental differential cross section for 90° (Fig. 5) is reproduced by the statistical-model calculation including the (*p*,*n*) outgoing channels. This fact confirms the approximations made in the CN cross-section estimate. Based on this fact, an attempt was made to separate the two reaction mechanisms competing for the excitation of the first state of Ar⁴⁰ by protons.

With this end in view, the total cross section was calculated by integrating the (*p*,*p'*) angular distributions on the state $Q = -1.46$ MeV, measured in the present work, and those previously given in the literature.¹⁻⁵

Taking into account the spread of the experimental data on the absolute value of the cross section, these data have been averaged over different energy intervals as follows: 5.20–6.23 MeV⁴; 6.45–7.77 MeV²⁻⁴; 8.5–10.5 MeV^{1,2}; 14.1 MeV^{2,5}; 16.9 MeV.⁵ The excitation function of the inelastic total cross section was also calculated in the framework of the statistical model,

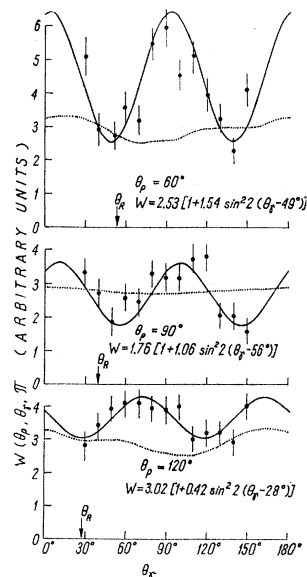


FIG. 6. The (*p*,*p'*γ) angular correlation between the protons inelastically scattered on the first Ar⁴⁰ excited state and the de-excitation gamma rays at $E_p = 5.8$ MeV. The solid curves represent the least-squares fits to the experimental data of functions (5) predicted by the DI mechanism, and the dashed curves, the predictions of the statistical model. θ_R is the classical recoil angle.

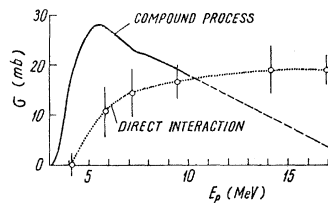


FIG. 7. A suggestion for the DI-CN competition in the total inelastic cross section for the excitation of the first state ($Q = -1.46$ MeV) of Ar^{40} . The CN contribution (solid curve) was computed on the basis of the statistical model up to $E_p = 10$ MeV and extrapolated at higher energies (dashed curve). The DI contribution was estimated by subtracting the CN cross section from the integrated experimental cross section. Every point of the DI curve represents the average over a given interval of the incident energy.

using formula (3) up to $E_p = 10$ MeV, the curve being then extrapolated at high energies.

In the calculation, averaged τ values were used. By subtracting the total CN cross section from the integrated experimental cross section, the probable value of the DI cross section was obtained. The result of this separation is shown in Fig. 7. The error bars were estimated taking into consideration the spread of the integrated cross section, the errors occurring in the integration, and a supposed 15% error in the estimate of the CN cross section.

The cross section for the direct process obtained in this way varies very little in the higher energy range, but a sharp decrease is noticed at energies below 6 MeV, situated in the vicinity of the Coulomb barrier.

At the energy 5.8 MeV, the DI cross section represents more than 25% of the inelastic total cross section. This fact is consistent with the data obtained in the angular-correlation experiment. Kokame and Fukunaga¹⁹ have obtained a similar variation of the DI cross section for the excitation of the low Al^{27} levels, with the difference that the sharp fall of the DI cross section occurs at an energy higher than the Coulomb barrier. But their method could not be applied in our case because of the lack of the angular distributions on the higher excited states for most of the bombarding energies, which could be employed as "monitors" in the estimation of the CN contribution with the aid of the $(2I+1)$ rule.

Even if we had these data at our disposal, at lower energies the method would be affected by large errors connected with the corrections due to Coulomb-barrier penetrability. For example at $E_p = 7.3$ MeV, in the case of the $Q = -3.23$ MeV state of Ar^{40} , the CN cross section predicted by the statistical model is smaller in the case

of a spin $I = 4+$ than in the case of $I = 2+$ (contrary to the $2I+1$ rule) because of the influence of the Coulomb barrier on the transmission coefficients. It is not clear in this case how the barrier corrections were to be applied, in view of the fact that the transmission coefficients contribute to formula (3) in a complicated way.

CONCLUSIONS

The experimental data presented in this work show the important contribution of the direct interaction in the explanation of the angular distributions and $(p, p_1\gamma)$ angular correlations on Ar^{40} .

The appearance of the direct mechanism, even at energies as low as 5.8 MeV, is a consequence of the relatively reduced weight of the compound mechanism, due to the competition of the (p, n) outgoing channels. If the (p, n) threshold were higher, the direct-mechanism contribution would not be smaller, but it would be difficult to detect in the presence of the CN process, which would have a larger cross section in this case. So the height of the (p, n) threshold acts as a gate in the process of making the DI mechanism evident.

Our data also suggest the possibility of using the statistical model to describe the part of the reaction which goes through the compound nucleus. This model proved to be effective in the explanation of the data of the $(p, p_1\gamma)$ angular correlation in the case of the medium-weight nuclei beginning with Ti^{48} , as shown in the analysis performed by Sheldon.¹⁰ From this point of view, Ar^{40} could be considered in the category of medium-weight nuclei.

Although the approximations made in the calculation of the contribution of the (p, n) channels can still be questioned, their utilization gives rise to a quantitative leap in the success of the statistical model in explaining the experimental cross-section data.

We think that the conclusions about the competition between the two reaction mechanisms, synthesized in Fig. 7, may be modified in their details, but not in their essentials.

The order of magnitude of the CN and the DI cross sections and the disappearance of the direct process at energies below the Coulomb barrier represent the chief results. It would be interesting to construct curves from Fig. 7, making calculations of the direct interaction in the DWBA formalism, the CN cross section being obtained by subtracting the DI cross section from the experimental one. The values obtained would give indications of the validity of the approximations we have made in the calculation of the CN cross section.